Published: Yasmin Mohamed Yousry, Kui Yao, Ayman Mahmoud Mohamed, Weng Heng Liew, Shuting Chen, and Seeram Ramakrishna, "Theoretical Model and Outstanding Performance from Constructive Piezoelectric and Triboelectric Mechanism in Electrospun PVDF Fiber Film," Advanced Functional Materials, doi.org/10.1002/adfm.201910592, online on 30 April 2020; Vol. 30, No. 25, 18 June 2020,1910592 (1 of 9).
Article type: Full Paper

Theoretical Model and Outstanding Performance from Constructive Piezoelectric and Triboelectric Mechanism in Electrospun PVDF Fiber Film

Yasmin Mohamed Yousry[1,2], Kui Yao[1], Ayman Mahmoud Mohamed[1], Weng Heng Liew[1,2], Shuting Chen[1], and Seeram Ramakrishna[2]*

Y. M. Yousry, Dr. K. Yao, A. M. Mohamed, Dr. S. Chen, Dr. W. H. Liew
Institute of Materials Research and Engineering, A*STAR (Agency for Science, Technology and Research), 2 Fusionopolis Way, Innovis, 138634, Singapore
E-mail: k-yao@imre.a-star.edu.sg
Y. M. Yousry, Prof. S. Ramakrishna
Department of Mechanical Engineering, National University of Singapore, 9 Engineering Drive 1, 117575, Singapore

Keywords: piezoelectric, triboelectric, polarization, PVDF, fibers

Flexible materials with high electromechanical coupling performance are highly demanded for wide applications for electromechanical sensors and transducers including mechanical energy harvesters. Here outstanding electromechanical performance is obtained in electrospun aligned PVDF fiber film. A theoretical model is developed from systematic theoretical analyses to clarify the underlying constructive piezoelectric-triboelectric mechanism in the polarized PVDF fiber films that well explain the experimental observations. The electrospinning process induces polarization alignment and thus tunes the electron affinity for PVDF fibers with different polarization terminals, which results in the constructive piezoelectric and triboelectric responses in the obtained PVDF fiber films. Extremely large effective piezoelectric performance properties are achieved in the direct piezoelectric measurements, reaching the maximum effective piezoelectric strain and voltage coefficients of -1065 pm V^{-1}, and -9178 V mm N^{-1}, respectively, at 100 Hz. In the converse piezoelectric measurements without as significant contribution from reversible triboelectric effect, the maximum effective

Published: Yasmin Mohamed Yousry, Kui Yao, Ayman Mahmoud Mohamed, Weng Heng Liew, Shuting Chen, and Seeram Ramakrishna, "Theoretical Model and Outstanding Performance from Constructive Piezoelectric and Triboelectric Mechanism in Electrospun PVDF Fiber Film," Advanced Functional Materials, doi.org/10.1002/adfm.201910592, online on 30 April 2020; Vol. 30, No. 25, 18 June 2020,1910592 (1 of 9).
piezoelectric strain and voltage coefficients are -166 pm V^{-1} and -1499 V mm N^{-1}, respectively. Our theoretical analyses and experimental results show the great potential of the electrospun aligned polar PVDF fiber material for various electromechanical device applications, particularly for mechanical energy harvesting.

1. Introduction

Self-powered wearable electronics are highly demanded for various emerging applications such as smart textiles, motion tracking, and health monitoring.[1,2] Energy harvesting technologies from the ambient environment or our body movement are of great importance to realize these self-powered systems. Fiber-based energy harvesting devices have the most desired features, such as light, soft, flexible, stretchable, and permeable, making them ideal to be employed as the interface platform among humans, environment, and machines.[1-4] In 2007, piezoelectric nanogenerator (PENG) was reported as a promising technology for generating electricity from ambient vibration based on the electromechanical coupling effect in piezoelectric materials.[5] From 2014, triboelectric nanogenerators (TENGs) have been studied to harvest mechanical energy based on electrostatic induction and triboelectrification of materials.[6] For improving the performance of electromechanical energy conversion devices, hybrid piezoelectric-triboelectric nanogenerators have been explored in the past few years to more effectively convert mechanical energy into electricity.[7-13] Piezoelectric effect refers to a change in electric polarization that is produced in a material without a center of structural symmetry when they are subjected to mechanical stresses,[14] while the triboelectric effect is the phenomenon that a material becomes electrically charged after it contacts with another material with different electron affiliation through friction, which is the coupling of contact electrification and electrostatic induction.[6] Although piezoelectricity and triboelectricity are

Published: Yasmin Mohamed Yousry, Kui Yao, Ayman Mahmoud Mohamed, Weng Heng Liew, Shuting Chen, and Seeram Ramakrishna, "Theoretical Model and Outstanding Performance from Constructive Piezoelectric and Triboelectric Mechanism in Electrospun PVDF Fiber Film," Advanced Functional Materials, doi.org/10.1002/adfm.201910592, online on 30 April 2020; Vol. 30, No. 25, 18 June 2020,1910592 (1 of 9).
two different mechanisms, they share many operational features in common for mechanical-to-electrical energy conversion. To date, the concept of hybrid piezoelectric-triboelectric generators is implemented with three composite structures: a 0-3 composite with polarized piezoelectric particles dispersed in another triboelectric matrix;[9] a 2-2 composite with one layer of piezoelectric and another layer of triboelectric material;[11] and a 2-2 composite with two inversely polarized piezoelectric layers.[7] However, these composites in the previous investigations have complex hybrid structures comprising different materials and/or different polarization configurations requiring electric poling process, as barriers for practical applications. Here we utilized both piezoelectric and triboelectric effects for achieving superior electromechanical conversion performance in electrospun polyvinylidene fluoride (PVDF) fibers as one single material system without additional electric poling treatment. It was shown that the electrospinning process induced the polarization orientation and thus tuned the electron affinity for the fibers with different polarization states at the surfaces, which result in constructive piezoelectric and triboelectric responses. Systematic analyses and various experimental measurements were conducted to establish a theoretical model to clarify the respective piezoelectric and triboelectric contributions.

2. Results and discussion

2.1. Device structure and surface morphology

PVDF is currently the most popularly used piezoelectric polymer material, and an introduction to PVDF polymer is given in **Supporting Information**. In this work, a PVDF fiber-based energy harvester with excellent flexibility was fabricated by sandwiching a film of aligned PVDF fibers between a bottom electrode (Al foil) and a top electrode (Cu tape), as shown in **Figure 1(a**), with the polarization direction being along the thickness of the fiber film,

Published: Yasmin Mohamed Yousry, Kui Yao, Ayman Mahmoud Mohamed, Weng Heng Liew, Shuting Chen, and Seeram Ramakrishna, "Theoretical Model and Outstanding Performance from Constructive Piezoelectric and Triboelectric Mechanism in Electrospun PVDF Fiber Film," Advanced Functional Materials, doi.org/10.1002/adfm.201910592, online on 30 April 2020; Vol. 30, No. 25, 18 June 2020,1910592 (1 of 9).
which is the same with the applied electric field direction during the electrospinning process.

As described in the schematic diagram of the electrospinning process, **Figure S1 (Supporting Information)**, a viscous PVDF solution was emitted from a Taylor cone at the needle tip and collected at the rotating drum covered with Al foil upon application of a high electrostatic field between the needle and the collector. The surface morphology of the obtained PVDF bundles of fibers is presented in Figure 1(b), 1(c), and 1(d) for the as-spun, annealed (at 135 °C), and melted (at 185 °C) bundles of PVDF fibers, respectively. The average diameter of the fibers decreases after annealing at 135 °C, while the porosity increases. Further thermal treatment at 185 °C, which is slightly above the melting temperature of PVDF homopolymer (178 °C), creates a partially fused network among the fibers without completely destroying the porous fibrous structure. The thickness of the annealed fiber film is 150 μm, while it shrinks to ~75 μm after melting, as shown in **Figure S2 (Supporting Information)**. Additional FESEM images with lower and higher magnification of the as-spun fibers are provided in **Figure S3 (Supporting Information),** showing that the fibers are uniform with very minor nanobeads. Obtaining the uniform PVDF fibers is highly desired for systematically investigating their functional properties and further clarifying their relationship to the structure.

Published: Yasmin Mohamed Yousry, Kui Yao, Ayman Mahmoud Mohamed, Weng Heng Liew, Shuting Chen, and Seeram Ramakrishna, "Theoretical Model and Outstanding Performance from Constructive Piezoelectric and Triboelectric Mechanism in Electrospun PVDF Fiber Film," Advanced Functional Materials, doi.org/10.1002/adfm.201910592, online on 30 April 2020; Vol. 30, No. 25, 18 June 2020,1910592 (1 of 9).

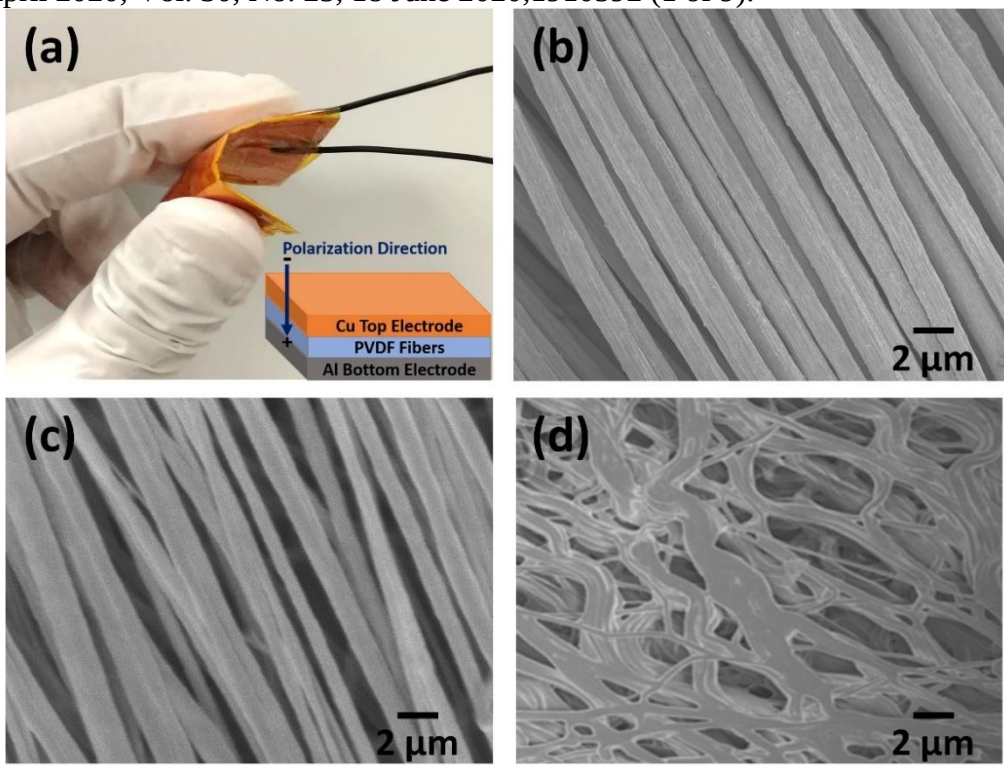

Figure 1. (a) A photo and schematic structure of the PVDF fiber energy harvesting device. FESEM image of bundles of fibers: **(b)** as-spun, **(c)** annealed at 135 ^{o}C, and **(d)** melted at 185 ^{o}C.

2.2. Crystalline structure

Figure 2(a) shows the attenuated total reflection (ATR) Fourier transform infrared (FTIR) spectra of the as-spun, annealed (at 135 °C), and melted (at 185 °C) PVDF fiber films. The distinctive absorption bands of the non-polar α phase are located at 764 and 975 cm^{-1}, while the distinctive absorption bands of the polar β phase located at 840, and 1276 cm^{-1}.[15] The FTIR spectrum of the as-spun PVDF fiber film shows pure β-phase content, which is related to in-situ poling and uniaxial stretching effects during the electrospinning process.[16] After annealing at 135 °C, the crystallinity is significantly enhanced as indicated by the increase in the intensity of the absorption bands of the polar β phase. When the annealed PVDF fiber film was further

Published: Yasmin Mohamed Yousry, Kui Yao, Ayman Mahmoud Mohamed, Weng Heng Liew, Shuting Chen, and Seeram Ramakrishna, "Theoretical Model and Outstanding Performance from Constructive Piezoelectric and Triboelectric Mechanism in Electrospun PVDF Fiber Film," Advanced Functional Materials, doi.org/10.1002/adfm.201910592, online on 30 April 2020; Vol. 30, No. 25, 18 June 2020,1910592 (1 of 9).
melted, the β phase crystallite after melting is recrystallized to the thermodynamically stable α phase, as indicated by the increased absorption bands of α phase and the suppressed absorption bands of β phase in the melted PVDF fiber film. Moreover, Figure 2(b) compares the X-ray diffraction (XRD) spectra of the as-spun, annealed, and melted PVDF fiber films. Characteristic XRD peaks with 2θ at 18.3°, 19.8°, and 20.1° corresponding to (100), (020), and (110) crystal planes of α phase, while 2θ at 20.8° corresponding to the sum of (110) and (200) plane reflections of β phase.[17] It is evidenced by an enhanced characteristic peak at 20.8° that the β phase is improved by the annealing treatment at 135 °C. While after melting at 185 °C, the crystallinity decreased significantly with the β phase disappeared, and the α phase is formed. The average crystallite size in the PVDF fibers was calculated using Scherrer's equation:[18]

$$D = \frac{K\lambda}{B\cos\theta} \qquad (1)$$

where D is the crystallite size, λ is the wavelength of X-ray radiation (0.15406 nm), B is the full width at half maximum (FWHM) of the most intense diffraction peak, θ is the angle of diffraction, k is a constant (having the value 0.89). The calculation results show that the crystallite size of the as-spun, annealed, and melted fiber films are 5.4 nm, 7.7 nm, and 6.1 nm, respectively, which indicates that annealing treatment of PVDF fibers enhances the crystallinity.

The crystalline β phase is characterized by a larger degree of polarization per unit cell compared with the α phase (theoretically zero), and a higher surface charge density may be obtained on the β-phase surface.[19] Hence, the highest surface charge density among the four crystalline phases can be obtained from the β-phase PVDF surface,[19] as will be discussed later.

Published: Yasmin Mohamed Yousry, Kui Yao, Ayman Mahmoud Mohamed, Weng Heng Liew, Shuting Chen, and Seeram Ramakrishna, "Theoretical Model and Outstanding Performance from Constructive Piezoelectric and Triboelectric Mechanism in Electrospun PVDF Fiber Film," Advanced Functional Materials, doi.org/10.1002/adfm.201910592, online on 30 April 2020; Vol. 30, No. 25, 18 June 2020,1910592 (1 of 9).

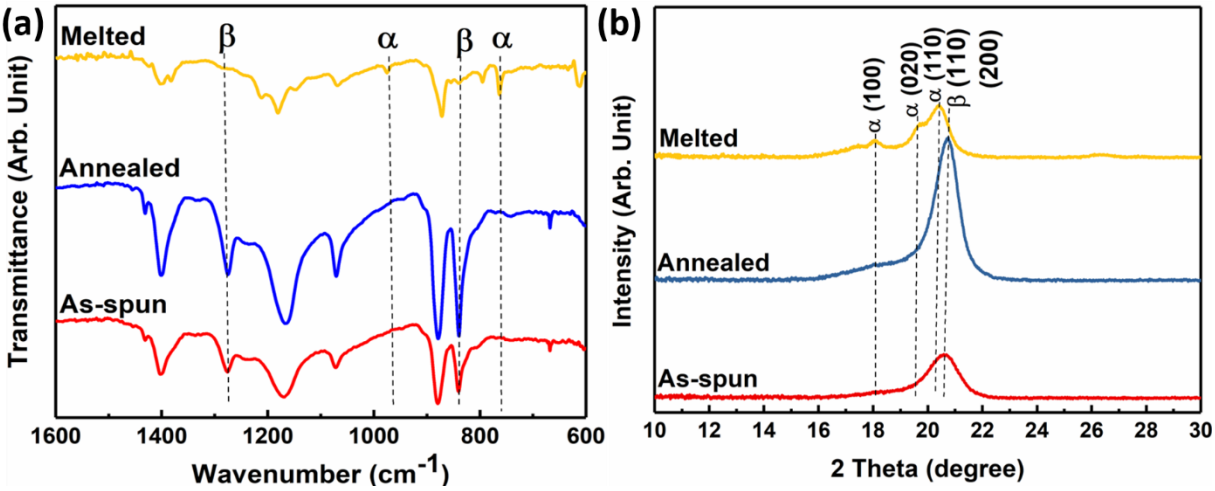

Figure 2: (a) FTIR spectra, and **(b)** XRD patterns of the as-spun, annealed (at 135 °C), and melted (at 185 °C) PVDF fiber films. The unmarked peaks in the FTIR spectra are common to both α and β phases.

2.3. Piezoelectric properties

The laser scanning vibrometer (LSV) testing for piezoelectric property [20] was conducted with a unipolar sine wave voltage of 15 V in amplitude at 1 kHz applied to the fiber films. **Figure 3(a), 3(b), and 3(c)** presents three-dimensional graphs of the instantaneous vibration data when the displacement magnitudes of the as-spun, annealed, and melted PVDF fiber films reach the maximum with the electric sine wave driving. The central protruding area is the electrically excited area under Au top electrode, whereas the adjacent flat area is the PVDF fibers without the top electrode. The average value over the top area rather than the highest point is used for calculating the effective piezoelectric strain coefficient $d_{33,\,LSV,}$ which is about -21, -166, and -8 pm V^{-1} for the as-spun, annealed, and melted PVDF fiber films, respectively, under the substrate clamping conditions.

Figure S4 (Supporting Information) presents the dielectric constant and dielectric loss of the as-spun, annealed, and melted PVDF fiber films, where the annealed PVDF fiber film

Published: Yasmin Mohamed Yousry, Kui Yao, Ayman Mahmoud Mohamed, Weng Heng Liew, Shuting Chen, and Seeram Ramakrishna, "Theoretical Model and Outstanding Performance from Constructive Piezoelectric and Triboelectric Mechanism in Electrospun PVDF Fiber Film," Advanced Functional Materials, doi.org/10.1002/adfm.201910592, online on 30 April 2020; Vol. 30, No. 25, 18 June 2020,1910592 (1 of 9).

possesses the highest dielectric constant with a maximum value of 13 (at 1 kHz) while maintaining the lowest dielectric loss over a broad frequency range up to 1 MHz. The as-spun and melted PVDF fiber films show reduced dielectric constant (9.6 and 4.4, respectively at 1 kHz) and higher dielectric loss, which is believed due to the lower crystallinity of the as-spun and melted fibers in addition to the degraded morphology of the melted fibers.

The corresponding effective piezoelectric voltage coefficient $g_{33,LSV}$ reaches -564, -1442, and -93 V mm N^{-1} for the as-spun, annealed, and melted fiber films, respectively. The enhanced crystallinity and higher β-phase content in the annealed PVDF fiber film lead to the outstanding piezoelectric strain and voltage coefficients. The smaller effective $d_{33,LSV}$ coefficient of the melted PVDF fibers is attributed to the loss of the β phase with the formation of α phase and thus polarization when annealed above Curie temperature, as previously reported.[21,22] It should be highlighted that the obtained effective piezoelectric strain and voltage coefficients of the annealed PVDF fiber films are much higher than the typical values for PVDF bulk films of -25 to -35 pm V^{-1}, and -320 to -452 V mm N^{-1}, respectively.[23]

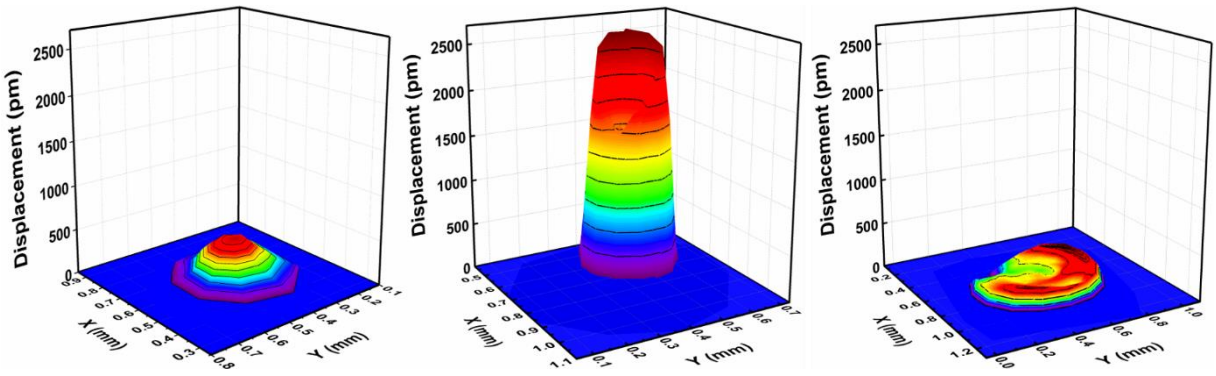

Figure 3. Three-dimensional graph of instantaneous vibration obtained when the dilatations of **(a)** as-spun, **(b)** annealed (at 135 °C), and **(c)** melted (at 185 °C) PVDF fiber films reach the maximum during the sine wave electric driving (15 V, at 1 kHz). The protruded central area is the electrically excited fiber films under the top Au electrode, whereas the adjacent flat area is the PVDF fiber films without the top electrode.

Published: Yasmin Mohamed Yousry, Kui Yao, Ayman Mahmoud Mohamed, Weng Heng Liew, Shuting Chen, and Seeram Ramakrishna, "Theoretical Model and Outstanding Performance from Constructive Piezoelectric and Triboelectric Mechanism in Electrospun PVDF Fiber Film," Advanced Functional Materials, doi.org/10.1002/adfm.201910592, online on 30 April 2020; Vol. 30, No. 25, 18 June 2020,1910592 (1 of 9).

The direct piezoelectric effect for converting mechanical input to electrical output was measured using a vibrational shaker apparatus to input the mechanical energy. The setup of measurement is shown in **Figure S5 (Supporting Information)**. The measurement was performed under frequencies of 10, 50, 100, 500, and 1000 Hz with corresponding acceleration amplitudes of 2.0, 2.5, 3.0, 4.1, and 4.9 g, respectively, at a constant input displacement of 1.2 mm. The output voltages at different amplitudes and frequencies are presented in **Figure 4(a) and 4(b)** for the annealed and melted PVDF fiber films, respectively, while we could not measure the performance of the as-spun fiber film due to delamination issue during the vibration. As the acceleration amplitude increases from 2.0 to 3.0 g (corresponding to the low frequencies of 10 to 100 Hz), the output voltage from the annealed PVDF fiber film increases rapidly from 0.8 to 3.6 V, as shown in Figure 4(a), indicating that our PVDF fiber film can be used as the functional material for mechanical energy harvesting or as a self-powered acceleration sensor through appropriate electrical design.[24,25] With further increasing the acceleration to 4.1 and 4.9g (corresponding to 500 and 1000 Hz), however, the output voltage drops to 0.8 and 0.95 V. For the melted PVDF fiber film, as the acceleration amplitude increases from 2.0 to 3.0 g (corresponding to the low frequencies of 10 to 100 Hz), the output voltage increases significantly as well from 0.4 to 2.1 V, while it drops to nearly zero at higher acceleration values in the high frequency range of 500 to 1000 Hz, as shown in Figure 4(b). The peak power density values are shown in Figure 4(c), and 4(d) for the annealed and melted PVDF fiber films, reaching a maximum of 0.21 $\mu W/cm^2$ and 0.08 $\mu W/cm^2$ at 100 Hz, respectively, while drops in lower and higher frequency ranges. The observed electrical output from the melted PVDF fiber film is not attributed to the intrinsic piezoelectric effect since the melted PVDF fiber film was characteristic of the non-polar α phase, and it also did not reversibly show substantial converse

Published: Yasmin Mohamed Yousry, Kui Yao, Ayman Mahmoud Mohamed, Weng Heng Liew, Shuting Chen, and Seeram Ramakrishna, "Theoretical Model and Outstanding Performance from Constructive Piezoelectric and Triboelectric Mechanism in Electrospun PVDF Fiber Film," Advanced Functional Materials, doi.org/10.1002/adfm.201910592, online on 30 April 2020; Vol. 30, No. 25, 18 June 2020,1910592 (1 of 9).

piezoelectric effect. Moreover, our measurements were performed at constant room temperature, which also excludes the pyroelectric response that requires a change in temperature to be effective. Instead, the electrical output from the melted PVDF fiber film can be attributed to electrostatic charge effect and change in the electrical potential as a result of triboelectric charge generation and change in the capacitance among the fibers corresponding to the gap variation during the vibration.[26,27] Moreover, it was reported that the output voltage from hybrid triboelectric-piezoelectric nanogenerators increases as the frequency of contact released increased, but the mechanism is unclear yet.[28-32] One distinct feature of piezoelectric output voltage is that the signal reverses its polarity when the measurement system is reversely connected.[33] However, in our work, signal polarity does not change when reversing the connection of the PVDF fiber films (either the annealed or the melted), which is not the typical behavior of intrinsic piezoelectric effect but rather associated with predominant electrostatic effect in the porous fiber structure.

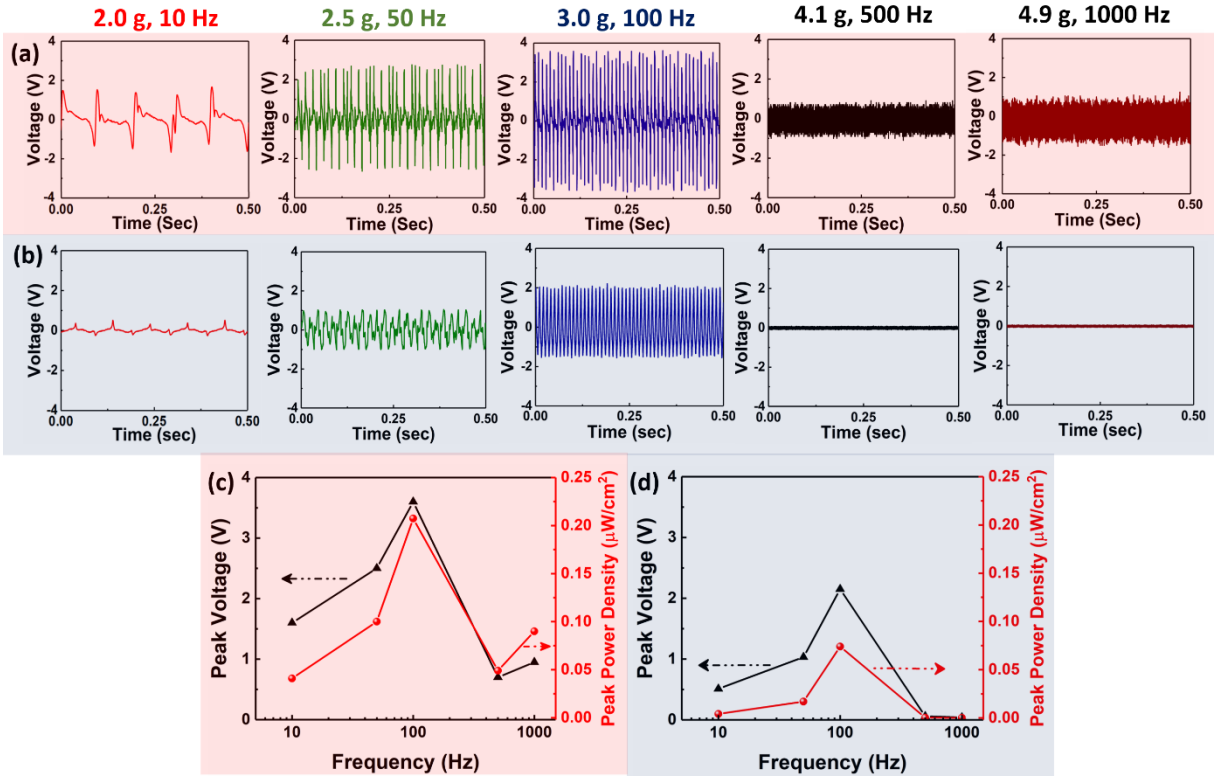

Published: Yasmin Mohamed Yousry, Kui Yao, Ayman Mahmoud Mohamed, Weng Heng Liew, Shuting Chen, and Seeram Ramakrishna, "Theoretical Model and Outstanding Performance from Constructive Piezoelectric and Triboelectric Mechanism in Electrospun PVDF Fiber Film," Advanced Functional Materials, doi.org/10.1002/adfm.201910592, online on 30 April 2020; Vol. 30, No. 25, 18 June 2020,1910592 (1 of 9).

Figure 4. Output voltages of **(a)** annealed (at 135 °C), and **(b)** melted (at 185 °C) PVDF fiber films measured at different frequencies, 10, 50, 100, 500, and 1000 Hz. Peak voltage and peak power density as a function of the frequency for **(c)** the annealed, and **(d)** melted PVDF fiber films. All the measurements were performed at a constant input displacement of 1.2 mm.

From the direct piezoelectric effect approach using the mechanical shaker, the effective piezoelectric strain coefficient $d_{33,\,Shaker}$ can be expressed as in Equation 2, with its derivation provided in the **Supporting Information**:[34]

$$V = -\frac{d_{33}\, M\, a\, h}{\varepsilon_{33}\, A} \qquad (2)$$

where V is the output voltage, M is the mass load (52 g), a is the acceleration amplitude (2.0, 2.5, 3.0, 4.1, 4.9 g), h is the film thickness (150 µm), ε_{33} is the dielectric permittivity (13 x 8.85 x 10^{-12} C^2 N^{-1} m^{-2}), and A is the area under the load 6.25 cm^2. After melting, the dielectric permittivity is (9.6 x 8.85 x 10^{-12} C^2 N^{-1} m^{-2}), the thickness of the PVDF fiber film decreased to 75 µm, and the area decreased to 1.56 cm^2, and accordingly the new mass load used was 12.5 g in order to maintain the same pressure during the measurement. Accordingly, the effective $d_{33,\,Shaker}$ and $g_{33,\,Shaker}$ values calculated from direct piezoelectric effect at different mechanical input, in comparison with the obtained values from the converse piezoelectric effect (LSV) at different voltages, are summarized in **Figure 5(a) and 5(b)**, respectively, for the annealed and melted PVDF fiber films. For the annealed PVDF fiber film, the effective $d_{33,\,LSV,\,Shaker}$ values obtained from both LSV and mechanical shaker measurements at 1 kHz are in the similar range, -160 and -172 pm V^{-1}, respectively, which are close to the maximum theoretical limit of -186 pm V^{-1} for PVDF; [35] while the effective $d_{33,\,Shaker}$ values at low frequencies are dramatically higher, -676 and -1065 pm V^{-1}, at 10 and 100 Hz, respectively. Similarly, the effective $g_{33,\,LSV,\,Shaker}$ values for the annealed PVDF fiber film obtained from both LSV and mechanical shaker

Published: Yasmin Mohamed Yousry, Kui Yao, Ayman Mahmoud Mohamed, Weng Heng Liew, Shuting Chen, and Seeram Ramakrishna, "Theoretical Model and Outstanding Performance from Constructive Piezoelectric and Triboelectric Mechanism in Electrospun PVDF Fiber Film," Advanced Functional Materials, doi.org/10.1002/adfm.201910592, online on 30 April 2020; Vol. 30, No. 25, 18 June 2020,1910592 (1 of 9).
measurements at 1 kHz are similar, -1374 and -1499 V mm N^{-1}, respectively; while the effective $g_{33,\ Shaker}$ values obtained from the mechanical shaker measurements at low frequencies, are extremely higher, -5875 and -9178 V mm N^{-1} for 10 and 100 Hz, respectively. However, for the melted PVDF fiber film without substantial polar phase, the effective $d_{33,\ LSV,\ Shaker}$ and $g_{33,\ LSV,\ Shaker}$ values measured at 1 kHz are less than -10 pm V^{-1} and -93 V mm N^{-1}, respectively, in all of the measurements with LSV and shaker while rather large effective $d_{33,\ Shaker}$ and $g_{33,\ Shaker}$ values of -697 and -8290 V mm N^{-1}, respectively, are observed at low frequencies with shaker. These results confirm that extrinsic factors contributed to the obtained electrical output during the direct piezoelectric measurement under the mechanical vibrations at low frequency. Here, the extrinsic factors may be related to triboelectric charge generation during mechanical vibration through contact electrification of the PVDF fibers. It should be highlighted that, the output voltage measured at low acceleration below 2.0 g was very low compared to results above 2.0 g as shown in **Figure S6 (Supporting Information**), which may be attributed to non-contact of the fibers at low acceleration without generating triboelectric charges, as will be discussed later with our established theoretical model.

Another direct piezoelectric measurement mode was conducted using a dynamic mechanical analyzer machine to evaluate the potentials of the obtained PVDF fiber films for mechanical energy harvesting applications under stretching in three different directions (fiber bundle radial, diagonal, and fiber axial directions **Figure S7 and Figure S8 (Supporting Information)**. The calculated effective $d_{31,\ Stretching}$ and $g_{31,\ Stretching}$ values are 14 pm V^{-1} and 128 mm V mm N^{-1}, 21 pm V^{-1} and 187 V mm N^{-1}, 37 pm V^{-1} and 328 V mm N^{-1}, respectively, in the fiber axial, diagonal, and bundle radial tension directions, respectively.

Published: Yasmin Mohamed Yousry, Kui Yao, Ayman Mahmoud Mohamed, Weng Heng Liew, Shuting Chen, and Seeram Ramakrishna, "Theoretical Model and Outstanding Performance from Constructive Piezoelectric and Triboelectric Mechanism in Electrospun PVDF Fiber Film," Advanced Functional Materials, doi.org/10.1002/adfm.201910592, online on 30 April 2020; Vol. 30, No. 25, 18 June 2020,1910592 (1 of 9).

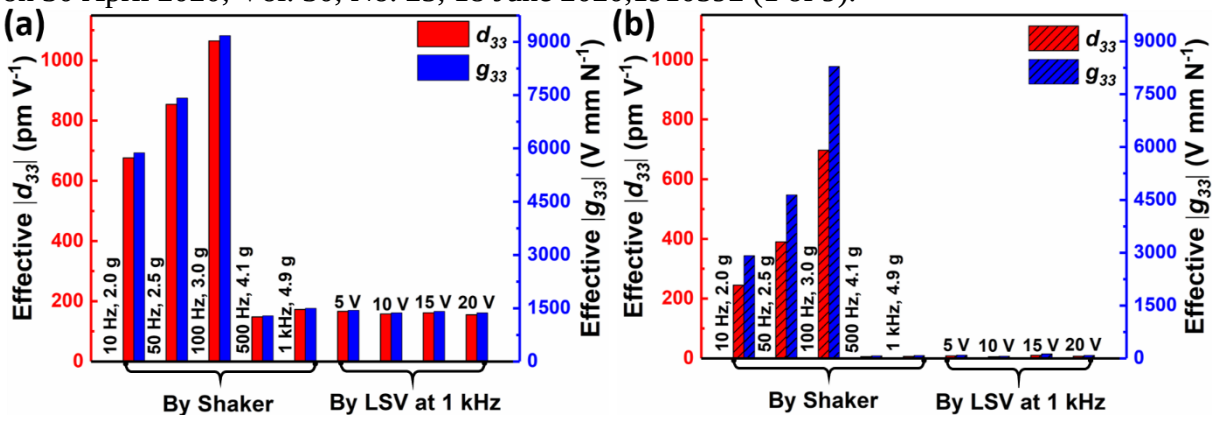

Figure 5. Comparison of the effective piezoelectric strain and voltage coefficients measured by LSV and shaker techniques for **(a)** annealed (at 135 °C), and **(b)** melted (at 185 °C) PVDF fiber films.

3. Theoretical Model and Analysis

For a polarized piezoelectric material lack of symmetric center, when mechanical stress is applied, the centers of the positive and negative charges shift relatively, leading to a net polarization and charge generation.[14,36,37] On the other hand, coupling of contact electrification and electrostatic induction between different materials leads to triboelectric charge generation.[6,36,38] Here we propose a model for describing a constructive piezoelectric-triboelectric mechanism in our polarized electrospun PVDF fibers with the significantly enhanced electrical output from mechanical input as observed.

Figure 6(a) illustrates the electrical generation of a piezoelectric material during one pressing and releasing cycle according to a conventional piezoelectric model. When a pressure applied onto the piezoelectric material, the dipolar momentum and overall polarization in the Pressed state are changed from the Original state, thus electrical potential or electric current I_{Piezo} is generated in response to the pressure. When the external pressure is partially released

Published: Yasmin Mohamed Yousry, Kui Yao, Ayman Mahmoud Mohamed, Weng Heng Liew, Shuting Chen, and Seeram Ramakrishna, "Theoretical Model and Outstanding Performance from Constructive Piezoelectric and Triboelectric Mechanism in Electrospun PVDF Fiber Film," Advanced Functional Materials, doi.org/10.1002/adfm.201910592, online on 30 April 2020; Vol. 30, No. 25, 18 June 2020,1910592 (1 of 9).
(Partially Released state), an opposite electrical potential change or current is induced. With the pressure released completely, it returns to the Original state.

Figure 6(b) illustrates charge generation through a triboelectric effect typically in two materials with different electron affinities. When the two charged triboelectric materials close to each other under applied pressure, an electrical potential change or I_{Tribo} is induced in response to the change in the electrostatic momentum or overall polarization (Partially Pressed state). When the two charged triboelectric materials contact each other with increased pressure, charge transfer takes place at the contact interface due to contact electrification (Pressed state). The different ability to gain or lose electrons due to the difference in their electron affinities leads to a triboelectric potential layer at the interface. Since the charges are only confined at the contact surfaces, charges with opposite signs coincide at almost the same plane, practically not generating electric potential difference between the two electrodes. Once the pressure is removed for separating the two triboelectric materials, an electrical potential difference is established between the two electrodes to minimize the energy created by the triboelectric charges, leading to an opposite potential between the two electrodes or a triboelectric current (Partially Released state). With the pressure released completely, the two materials return to their respective Original states.

Published: Yasmin Mohamed Yousry, Kui Yao, Ayman Mahmoud Mohamed, Weng Heng Liew, Shuting Chen, and Seeram Ramakrishna, "Theoretical Model and Outstanding Performance from Constructive Piezoelectric and Triboelectric Mechanism in Electrospun PVDF Fiber Film," Advanced Functional Materials, doi.org/10.1002/adfm.201910592, online on 30 April 2020; Vol. 30, No. 25, 18 June 2020,1910592 (1 of 9).

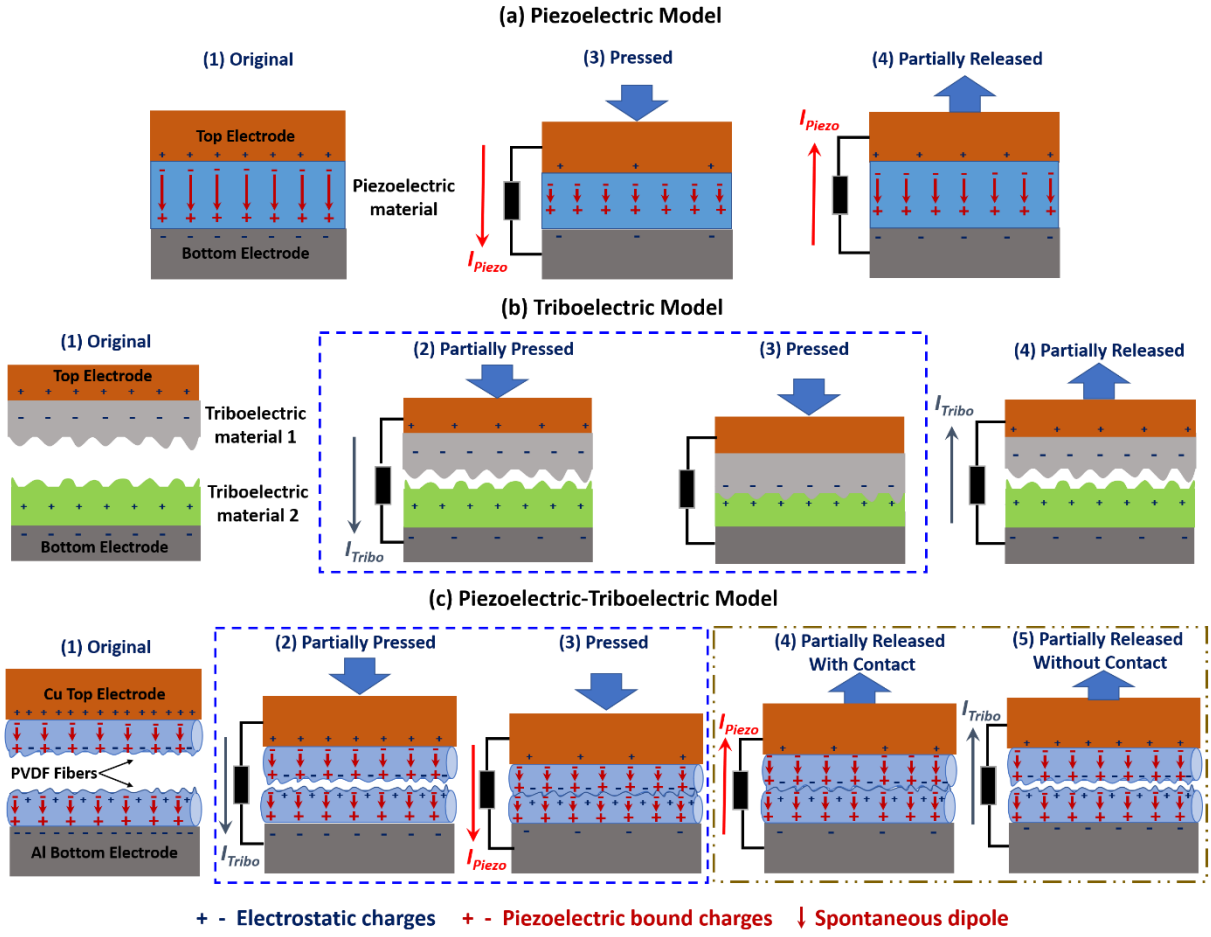

Figure 6. Theoretical models for mechanical to electrical conversion mechanisms through **(a)** piezoelectric effect in a piezoelectric material, **(b)** triboelectric effect in two different dielectric materials, and **(c)** constructive piezoelectric-triboelectric effect in PVDF fibers with aligned electrical polarization.

Figure 6(c) illustrates our proposed charge generation mechanism through a constructive piezoelectric and triboelectric effects in electrospun polarized PVDF fibers as one single material. The fiber film device in the model contains four parts: the PVDF fibers, the gap between the fibers representing the pore, Al foil as the bottom electrode, and copper tape as the top electrode. The electrospun fibers have the oriented spontaneous polarization, and electrostatic charges in the electrodes and fibers as shown in the Original state, including the charges screening the spontaneous polarization and the charges from triboelectric effect

Published: Yasmin Mohamed Yousry, Kui Yao, Ayman Mahmoud Mohamed, Weng Heng Liew, Shuting Chen, and Seeram Ramakrishna, "Theoretical Model and Outstanding Performance from Constructive Piezoelectric and Triboelectric Mechanism in Electrospun PVDF Fiber Film," Advanced Functional Materials, doi.org/10.1002/adfm.201910592, online on 30 April 2020; Vol. 30, No. 25, 18 June 2020,1910592 (1 of 9).
happened previously at fiber interfaces. When the fibers with the different dipole orientation and hence different electron affinity come into contact, charges transfer between the adjacent fibers (**Figure S9, Supporting Information)**. It has been reported that the intrinsic dipole moment alters the surface potential level of PVDF film, which can modulate the surface charge transfer tendency between PVDF film and the other type of material in contact. [11, 39-41] Additional opposite electrostatic charges are thus induced in the electrodes due to the triboelectric charges in polarized PVDF fibers. With pressure applied, the PVDF fibers become close to each other, and an electrical potential change or I_{Tribo} is induced in response to the change in the electrostatic momentum (Partially Pressed state). When the PVDF fibers contact each other with further increased pressure, deformation of the solid piezoelectric fibers leads to change in the spontaneous dipolar momentum and overall polarization, thus a piezoelectric potential or piezoelectric current I_{Piezo} is generated in response to the increased pressure, and the I_{Piezo} is in the same direction as I_{Tribo} (Pressed state as illustrated in Figure 6(c) (3)). When the external pressure is partially released (Partially Released with Contact state), an opposite piezoelectric potential change or piezoelectric current is induced, thus the direction of I_{Piezo} will become opposite. Once the pressure is removed to the extent for separating the PVDF fibers, an electrical potential difference is established between the two electrodes to minimize the energy created by the triboelectric charges, leading to an opposite triboelectric current, constructively enhance the opposite piezoelectric current (Partially Released without Contact state). With the pressure released completely, the PVDF fibers return to the Original state. According to the model, the electrical output from the triboelectric and piezoelectric effects are not completely synchronized in response to the mechanical input. For the triboelectric output, the electrical output is generated substantially either when the two fibers are in Partially Pressed or Partially Released states. The triboelectric effect does not produce substantial electrical

Published: Yasmin Mohamed Yousry, Kui Yao, Ayman Mahmoud Mohamed, Weng Heng Liew, Shuting Chen, and Seeram Ramakrishna, "Theoretical Model and Outstanding Performance from Constructive Piezoelectric and Triboelectric Mechanism in Electrospun PVDF Fiber Film," Advanced Functional Materials, doi.org/10.1002/adfm.201910592, online on 30 April 2020; Vol. 30, No. 25, 18 June 2020,1910592 (1 of 9).
output when the two surfaces stay in contact, while the piezoelectric effect becomes significant with the deformation in the solid occurs after the contact is achieved with a pressure in the Pressed or Partially Released with Contact state. However, it should be pointed out that in a practical PVDF fiber film, there are many fibers and different sizes of gaps among the fibers, Partially Pressed and Pressed states, Partially Released and Released states, always co-exist at different locations across the material under a dynamic mechanical input.

Our above-stated piezoelectric-triboelectric model as shown in Figure 6(b) and 6(c) can well explain the observed results from the annealed and melted PVDF fiber films during the shaker measurements. The contributions of the triboelectric and piezoelectric effects can be analyzed with our theoretical model by examining the details of the output voltage waveform in response to the mechanical release-press cycle for the annealed and melted PVDF fiber films, as shown in **Figure S10 (Supporting Information)**. At low acceleration value of 2.0 g at 10 Hz which is not adequate to generate substantial solid deformation in the fibers, the electric output is mainly attributed to the triboelectric effect with only very minor contribution from the piezoelectric effect. In this case, the voltage waveform is not of a sine wave in phase with the vibration, i.e., the maximum output does not coincide with the vibration maximum, as shown in Figure S10 (a) (Supporting Information). This is consistent with the occurrence of I_{Tribo} at the Partially Pressed and Partially Released state without physical contact, as marked in Figure 6(b) (2) (4) and 6(c) (2) and (5), accordingly. When the acceleration increases from 2.0 to 3.0 g at 100 Hz, the electric output of the annealed PVDF fiber film increases due to the increased contact area for enhanced triboelectric effect and the increased deformation in the solid fibers for enhanced contributions from intrinsic in-phase piezoelectric effect, as shown in Figure S10 (b) (Supporting Information). As the electric output is still predominated by the triboelectric contribution, the maximum voltage output does not coincide with the acceleration maximum.

Published: Yasmin Mohamed Yousry, Kui Yao, Ayman Mahmoud Mohamed, Weng Heng Liew, Shuting Chen, and Seeram Ramakrishna, "Theoretical Model and Outstanding Performance from Constructive Piezoelectric and Triboelectric Mechanism in Electrospun PVDF Fiber Film," Advanced Functional Materials, doi.org/10.1002/adfm.201910592, online on 30 April 2020; Vol. 30, No. 25, 18 June 2020,1910592 (1 of 9).
With further increasing the acceleration to 4.1 and 4.9 g, typical sine wave voltage outputs in phase with the acceleration are observed, as shown in Figure S10 (c), and (d) (Supporting Information). The underlying mechanism is that such a large acceleration results in large area physical contacts and solid deformation in the fibers, and thus the electrical output is predominated by the intrinsic piezoelectric effect rather than the triboelectric effect, according to our theoretical model as illustrated in Figure 6(c) (3) and (4), corresponding to the states of Pressed and Partially Released with Contact (note I_{piezo} marked in the drawings instead of I_{Tribo}). In these states under large acceleration at high frequency, the triboelectric effect becomes not significant because almost all the fibers are contacted without generating substantial triboelectric charges. It is interesting to note that for the non-polar melted PVDF fiber film, no any substantial electrical output is generated in Figure S10 (c) and (d) (Supporting Information) since it is not ferroelectric or intrinsic piezoelectric, although substantial electric output is generated through triboelectric effect under low acceleration at low frequency (Figure S10 (b) (Supporting Information)).

Oscillating voltage tails corresponding to the triboelectric effect under low mechanical input at low frequency are noted in Figure S10 (a) and (b) (Supporting Information), which may be related to high order vibration in the fibers without physical contact or the porous structure. The voltage output peaks in the pressed period are higher compared to the peaks in the released period from the triboelectric effect (Figure S10 (a) and (b) (Supporting Information)). The reason may be attributed to the slower rate for the soft fibers to be separated back to their original state than the contact process under press. In contrast, these waveform irregularities are not present in the intrinsic piezoelectric effect from the deformation in the solid fibers (Figure S10 (c) and (d) (Supporting Information)).

Published: Yasmin Mohamed Yousry, Kui Yao, Ayman Mahmoud Mohamed, Weng Heng Liew, Shuting Chen, and Seeram Ramakrishna, "Theoretical Model and Outstanding Performance from Constructive Piezoelectric and Triboelectric Mechanism in Electrospun PVDF Fiber Film," Advanced Functional Materials, doi.org/10.1002/adfm.201910592, online on 30 April 2020; Vol. 30, No. 25, 18 June 2020,1910592 (1 of 9).

All the measurement results in the electrical outputs in Figure 4 and Figure S10 (Supporting Information) show the constructive contributions from triboelectric and piezoelectric effect, with triboelectric effect is predominant under low acceleration at low frequency and intrinsic piezoelectric effect under high acceleration at high frequency, which can be well explained with our theoretical model in Figure 6.

The constructive contributions of the piezoelectric and triboelectric effects in the annealed PVDF fiber film lead to the outstanding effective piezoelectric performance achieved through the direct piezoelectric measurements by the mechanical shaker at acceleration value of 3.0 g, reaching maximum effective $d_{33,\ Shaker}$ and $g_{33,\ Shaker}$ values of -1065 pm V^{-1}, and -9178 V mm N^{-1}, respectively, as shown in Figure 5(a). While in the converse piezoelectric measurements by LSV at 1 kHz, the functioning mechanism is different, without significant contribution from reversible triboelectric effect, the maximum effective $d_{33,\ LSV}$ and $g_{33,\ LSV}$ values of -166 pm V^{-1} and -1499 V mm N^{-1}, respectively, as shown in Figure 5(a).

On the other hand, in the case of the non-polar melted PVDF fibers, where without any intrinsic piezoelectric effect, the maximum effective $d_{33,\ Shaker}$ and $g_{33,\ Shaker}$ values of -697 pm V^{-1} and -8290 V mm $N^{-1}$are observed with shaker measurements, respectively, as shown in Figure 5(b), while the effective $d_{33,\ LSV,\ Shaker}$ and $g_{33,\ LSV,\ Shaker}$ values are as low as -5 pm V^{-1} and -62 V mm N^{-1} by LSV measurements at 1 kHz, respectively, as shown in Figure 5(b).

Our theoretical analyses and experimental results show the great potential of the PVDF fiber films with the constructive piezoelectric-triboelectric contributions for energy harvesting applications. **Figure S11** presents an energy harvesting demonstration, in which the annealed PVDF fiber film is used for powering an LED under mechanical vibration of 3.0 g at 100 Hz.

4. Conclusion

Published: Yasmin Mohamed Yousry, Kui Yao, Ayman Mahmoud Mohamed, Weng Heng Liew, Shuting Chen, and Seeram Ramakrishna, "Theoretical Model and Outstanding Performance from Constructive Piezoelectric and Triboelectric Mechanism in Electrospun PVDF Fiber Film," Advanced Functional Materials, doi.org/10.1002/adfm.201910592, online on 30 April 2020; Vol. 30, No. 25, 18 June 2020,1910592 (1 of 9).

In this work, we presented outstanding electromechanical performance obtained in electrospun aligned PVDF fiber film, and developed a theoretical model from systematic theoretical analyses to clarify the underlying constructive piezoelectric-triboelectric mechanism in the polarized PVDF fiber films that contributed to the experimental observations. The electrospinning process induced polarization alignment and thus tuned the electron affinity for PVDF fibers with different polarization terminals, which resulted in the constructive piezoelectric and triboelectric responses in the obtained PVDF fiber films. In the direct piezoelectric measurements, the asymmetric triboelectric response predominates the electric output under low acceleration at low frequency, not in phase with the vibration, when the fibers are in Partially Pressed or Partially Released state without substantial physical contact; while the symmetric intrinsic piezoelectric response predominates the output, in phase with the vibration, under high acceleration at high frequency, corresponding to the states of Pressed and Partially Released with contact in which deformation in the solid fibers is substantial. Extremely large effective piezoelectric performance properties were achieved in the direct piezoelectric measurements with mechanical shaker, reaching the maximum effective strain and voltage coefficients ($d_{33,\,Shaker}$ and $g_{33,\,Shaker}$) of -1065 pm V^{-1}, and -9178 V mm N^{-1}, respectively, with 3 g acceleration at 100 Hz. In the converse piezoelectric measurements by LSV, without a significant contribution from reversible triboelectric effect, the maximum effective $d_{33,\,LSV}$ and $g_{33,\,LSV}$ values were -166 pm V^{-1} and -1499 V mm N^{-1}, respectively. Our theoretical analyses and experimental results show the great potential of the electrospun aligned polar PVDF fiber material for various electromechanical sensors and transducers applications, particularly for mechanical energy harvesting.

5. Experimental Section

Published: Yasmin Mohamed Yousry, Kui Yao, Ayman Mahmoud Mohamed, Weng Heng Liew, Shuting Chen, and Seeram Ramakrishna, "Theoretical Model and Outstanding Performance from Constructive Piezoelectric and Triboelectric Mechanism in Electrospun PVDF Fiber Film," Advanced Functional Materials, doi.org/10.1002/adfm.201910592, online on 30 April 2020; Vol. 30, No. 25, 18 June 2020,1910592 (1 of 9).

Materials: PVDF precursor solution was prepared by dissolving PVDF (540,000 MW, Sigma-Aldrich) in a solvent composed of 80 wt% dimethylformamide (DMF, TEDIA) and 20 wt% acetone (J. T. Baker). The solution was heated at 55 °C in silicone oil bath for 2 hours to completely dissolve the polymer until getting a clear transparent solution.

Electrospinning deposition: The PVDF solution was loaded in a plastic syringe capped with a 21-gauge stainless steel needle (inner diameter = 0.82 mm). A high voltage of 15 kV was applied to the needle through a DC power supply (Gamma High Voltage, AU-30P1-L220V, Japan). The solution was injected from the needle at a constant rate of 0.5 mL/h with a syringe pump (SP100IZ Syringe Pump, 789100W, U.S.A). A rotating cylinder made of a metallic plate covered with an Al foil was grounded and used as the fiber collector with a rotating speed of 1500 rpm for obtaining the aligned fiber film. The wet fibers were dried on a hotplate at 100 °C for 10 minutes then annealed at 135 °C for 12 hours in an oven. The thickness of the films was fixed at 150 μm by controlling the deposition parameters of the electrospinning process. To exclude the intrinsic piezoelectric effect as a control for comparison, the annealed fibers were further melted at 185 °C for 3 minutes at a hotplate to form non-polar melted sample.

Characterizations: The surface morphology was examined using a field emission scanning electron microscopy (FESEM, JSM-6700F, JEOL). The crystalline structure analysis was performed at room temperature using X-ray diffraction (XRD system D8-ADVANCE, Bruker AXS GmbH, Karlsruhe, Germany) and Fourier transform infrared (FTIR spectroscopy Spectrum 2000, Perkin Elmer). The frequency-dependent dielectric properties of the films were analyzed by an impedance analyzer (Agilent 4294A). The effective converse piezoelectric property was determined with a laser scanning vibrometer (OFV-3001-SF6, PolyTech GmbH, Germany). The direct piezoelectric property was characterized by a vibrational shaker (TIRA TV 51110 from TIRA GmbH) in which a power amplifier (TIRA BAA 120) was used to excite

Published: Yasmin Mohamed Yousry, Kui Yao, Ayman Mahmoud Mohamed, Weng Heng Liew, Shuting Chen, and Seeram Ramakrishna, "Theoretical Model and Outstanding Performance from Constructive Piezoelectric and Triboelectric Mechanism in Electrospun PVDF Fiber Film," Advanced Functional Materials, doi.org/10.1002/adfm.201910592, online on 30 April 2020; Vol. 30, No. 25, 18 June 2020,1910592 (1 of 9).
the shaker, and an accelerator (4525B-51049 from Brüel and Kjær) was used to measure the acceleration. The electrospun PVDF fiber film was sandwiched between bottom and top electrodes with a mass load (weight of 0.054 Kg) to generate electrical output in response to mechanical vibration from the shaker driven by a power amplifier and function generator. The voltage outputs were recorded using a Tektronix P6139B oscilloscope over a matched loading resistance of 10 MΩ. A dynamic mechanical analyzer machine (DMA Q800 from TA Instruments) was used to apply a dynamic tensile strain with the strain amplitude ramped from 0 to 20 %, under a pre-load of 0.5 N at 1 Hz. The PVDF fiber film (0.6×3 cm^2) was sandwiched between two layers of sputtered gold; then it was clamped and stretched using the DMA machine. During tension, the output voltage was recorded using a Tektronix P6139B oscilloscope while varying the stretching strain of the PVDF fiber film.

Supporting Information

Supporting Information is available from the Wiley Online Library or from the author.

Acknowledgments

The authors acknowledge the research grant support in part by Singapore Maritime Institute under the Maritime Sustainability R&D Programme, Project ID: SMI-2015-MA-07 (SC25/16-7P1125). The authors from IMRE acknowledge the support from the National Research Foundation Competitive Research Programme of Singapore, NRF-CRP15-2015-04, (IMRE/16-9P1122).

The work was designed by K. Yao, Y. M. Yousry and S. Ramakrishna. Preparing materials and carrying out experiments were done by Y. M. Yousry. K. Yao and Y. M. Yousry conducted the theoretical analysis on the results. W. H. Liew, A. M. Mohamed and S. Chen assisted in the electrical characterization. A. M. Mohamed assisted in the mechanical characterization. All the authors contribute to writing and revising the manuscript.

References

[1] X. Tao, *Acc. Chem. Res*. **2019**, *52*, 307.

[2] K. Dong, X. Peng, Z. L. Wang, *Adv. Mater*. **2019**, 1902549, 1.

Published: Yasmin Mohamed Yousry, Kui Yao, Ayman Mahmoud Mohamed, Weng Heng Liew, Shuting Chen, and Seeram Ramakrishna, "Theoretical Model and Outstanding Performance from Constructive Piezoelectric and Triboelectric Mechanism in Electrospun PVDF Fiber Film," Advanced Functional Materials, doi.org/10.1002/adfm.201910592, online on 30 April 2020; Vol. 30, No. 25, 18 June 2020,1910592 (1 of 9).

[3] M. Xie, K. Hisano, M. Zhu, T. Toyoshi, M. Pan, S. Okada, O. Tsutsumi, S. Kawamura, C. Bowen, *Adv. Mater. Technol*. **2019**, *4*, 1800626.

[4] Y. M. Yousry, K. Yao, S. Chen, W. H. Liew, and S. Ramakrishna, *Adv. Electron. Mater.* **2018**, *4*, 1700562.

[5] Y. Gao, Z. L. Wang, *Nano Lett.* **2007**, *7*, 2499.

[6] Z. L. Wang, *Faraday Discuss*. **2014**, *176*, 447.

[7] L. Lapcinskis, K. Malnieks, A. Linarts, J. Blums, K. Janis Smits, M. Jarvekulg, M. Knite, A. Sutka, *ACS Appl. Energy Mater*. **2019**, *2*, 4027.

[8] S. Chen, X. Tao, W. Zeng, B. Yang, S. Shang, *Adv. Energy Mater.* **2017**, *7*, 1601569.

[9] G. Suo, Y. Yu, Z. Zhang, S. Wang, P. Zhao, J. Li, X. Wang, *ACS Appl. Mater. Interfaces* **2016**, *8*, 34335.

[10] A. R. Chowdhury, A. M. Abdullah, I. Hussaina, J. Lopez, D. Cantua, S. K. Gupta, Y. Mao, S. Danti, M. J. Uddin, *Nano Energy* **2019**, *61*, 327.

[11] S. Cheon, H. Kang, H. Kim, Y. Son, J. Y. Lee, H. J. Shin, S. W. Kim, J. H. Cho, *Adv. Funct. Mater.* **2018**, *28*, 1703778.

[12] X. Wang, B. Yang, J. Liu, C. Yang, *J. Mater. Chem. A* **2017**, *5*, 1176.

[13] Y. Guo, X. S. Zhang, Y. Wang, W. Gong, Q. Zhang, H. Wang, J. Brugger, *Nano Energy* **2018**, *48*, 152.

[14] K. Uchino, *Advanced Piezoelectric Materials: Science and Technology*, Woodhead, Duxford, United Kingdom **2017**.

[15] X. Ma, J. Liu, C. Ni, D. C. Martin, D. B. Chase, J. F. Rabolt, *ACS Macro Lett.* **2012**, *1*, 428.

[16] Y. Ahn, J. Y. Lim, S. M. Hong, J. Lee, J. Ha, H. J. Choi, Y. Seo, *J. Phys. Chem. C* **2013**, *117*, 11791.

Published: Yasmin Mohamed Yousry, Kui Yao, Ayman Mahmoud Mohamed, Weng Heng Liew, Shuting Chen, and Seeram Ramakrishna, "Theoretical Model and Outstanding Performance from Constructive Piezoelectric and Triboelectric Mechanism in Electrospun PVDF Fiber Film," Advanced Functional Materials, doi.org/10.1002/adfm.201910592, online on 30 April 2020; Vol. 30, No. 25, 18 June 2020,1910592 (1 of 9).

[17] R. Gregorio, N. C. P. S. Nociti, *J. Phys. D: Appl. Phys.* **1995**, *28*, 432.

[18] P. Scherrer, *Math. Phys. Kl.* **1918**, *2*, 98.

[19] A. J. Lovinger, *Science* **1983**, *220*, 1115.

[20] K. Yao, F. E. H. Tay, *IEEE Trans. Ultrason. Ferroelectr. Freq. Control* **2003**, 50, 113.

[21] L. Ruan, X. Yao, Y. Chang, L. Zhou, G. Qin, X. Zhang, *Polymers* **2018**, *10*, 228.

[22] X. Wang, F. Sun, G. Yin, Y. Wang, B. Liu, M. Dong, *Sensors* **2018**, *18*, 330.

[23] C. Wan, C. R. Bowen, *J. Mater. Chem. A* **2017**, *5*, 3091.

[24] S. C. Lai, K. Yao, C. Y. Tan, *IEEE Sensors Journal* **2016**, *16*, 7841.

[25] H. Yu, J. Zhou, L. Deng, Z. Wen, *Sensors* **2014**, *14*, 3323.

[26] H. Tian, S. Ma, H. M. Zhao, C. Wu, J. Ge, D. Xie, Y. Yang, T. L. Ren, *Nanoscale* **2013**, *5*, 8951.

[27] H. Zou, Y. Zhang, L. Guo, P. Wang, X. He, G. Dai, H. Zheng, C. Chen, A. C. Wang, C. Xu, Z. L. Wang, *Nat. Commun.* **2019**, *10*, 1427.

[28] X. Wang, B. Yang, J. Liu, Y. Zhu, C. Yang, Q. He, *Sci. Rep.* **2016**, *6*, 1.

[29] W. Wang, J. Xu, H. Zheng, F. Chen, K. Jenkins, Y. Wu, H. Wang, W. Zhang, R. Yang, *Nanoscale* **2018**, *10*, 14747.

[30] Y. Zhang, Z. Zhou, L. Sun, Z. Liu, X. Xia, T. H. Tao, *Adv. Mater*. **2018**, *1805722*, 1.

[31] X. S. Zhang, M. D. Han, R. X. Wang, F. Y. Zhu, Z. H. Li, W. Wang, H. X. Zhang, *Nano Lett.* **2013**, *13*, 1168.

[32] B. Yang, W. Zeng, Z. H. Peng, S. R. Liu, K. Chen, X. M. Tao, *Adv. Energy Mater*. **2016**, *1600505*, 1.

[33] V. Bhavanasi, V. Kumar, K. Parida, J. Wang, P. S. Lee, *ACS Appl. Mater. Interfaces* **2016**, *8*, 521.

[34] J. Fialka, P. Benes, *IEEE Trans. Instrum. Meas.* **2013**, *62*, 1047.

Published: Yasmin Mohamed Yousry, Kui Yao, Ayman Mahmoud Mohamed, Weng Heng Liew, Shuting Chen, and Seeram Ramakrishna, "Theoretical Model and Outstanding Performance from Constructive Piezoelectric and Triboelectric Mechanism in Electrospun PVDF Fiber Film," Advanced Functional Materials, doi.org/10.1002/adfm.201910592, online on 30 April 2020; Vol. 30, No. 25, 18 June 2020,1910592 (1 of 9).
[35] K. Tashiro, H. Tadokoro, *Macromolecules* **1983**, *16*, 961.

[36] L. Huang, S. Lin, Z. Xu, H. Zhou, J. Duan, B. Hu, J. Zhou, *Adv. Mater.* **2019**, *1902034*, 1.

[37] K. Dong, X. Peng, Z. L. Wang, *Adv. Mater.* **2019**, *1902549*,1.

[38] Y. J. Kim, J. Lee, S. Park, C. Park, C. Park, H. J. Choi, *RSC Adv*., **2017**, *7*, 49368.

[39] R. Hinchet, W. Seung, S. W. Kim, *Chem Sus Chem* **2015**, *8*, 2327.

[40] M. A. Khan, M. A. Nadeem, H. Idriss, *Surf. Sci. Rep.* **2016**, *71*, 1.

[41] P. Bai, G. Zhu, Y. S. Zhou, S. Wang, J. Ma, G. Zhang, Z. L. Wang, *Nano Res.* 2**014**, *7*, 990.

Outstanding electromechanical conversion performance is achieved through constructive piezoelectric and triboelectric effects in aligned electrospun PVDF fibers. A theoretical model is developed from systematic theoretical analyses to clarify the constructive piezoelectric-triboelectric mechanism and explain the giant electric output in response to

Published: Yasmin Mohamed Yousry, Kui Yao, Ayman Mahmoud Mohamed, Weng Heng Liew, Shuting Chen, and Seeram Ramakrishna, "Theoretical Model and Outstanding Performance from Constructive Piezoelectric and Triboelectric Mechanism in Electrospun PVDF Fiber Film," Advanced Functional Materials, doi.org/10.1002/adfm.201910592, online on 30 April 2020; Vol. 30, No. 25, 18 June 2020,1910592 (1 of 9).
vibration in the polarized PVDF fiber material, with great potential for mechanical energy harvesting application.

Keyword: piezoelectric, triboelectric, polarization, PVDF, fibers

Y. M. Yousry, K. Yao, A. M. Mohamed, W. H. Liew, S. Chen, and S. Ramakrishna*
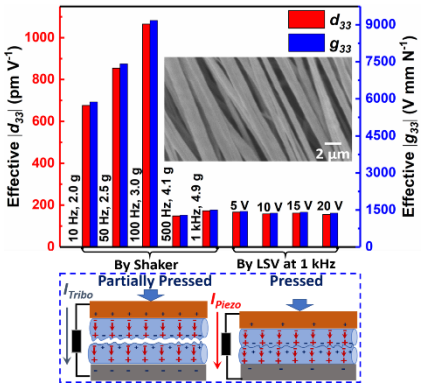
Theoretical Model and Outstanding Performance from Constructive Piezoelectric and Triboelectric Mechanism in Electrospun PVDF Fiber Film